Available online at www.sciencedirect.com
ScienceDirect
Polymer 48 (2007) 5721–5733
polymer
www.elsevier.com/locate/polymer

Dielectric and thermal behavior of liquid crystalline comb-like polybutadiene-diols with mesogenic groups in side chains

A. Jigounov [a], Z. Sedláková [b], R. Kripotou [c], P. Pissis [c], J. Nedbal [a], J. Baldrian [b], M. Ilavský [a,b,*]

[a] *Faculty of Mathematics and Physics, Charles University, 180 00 Prague 6, Czech Republic*
[b] *Institute of Macromolecular Chemistry, Academy of Sciences of the Czech Republic 162 06 Prague 6, Czech Republic*
[c] *School of Applied Mathematics and Physics, National Technical University of Athens, 157 80 Athens, Greece*

Received 10 May 2007; received in revised form 28 June 2007; accepted 2 July 2007
Available online 20 July 2007

Abstract

Ordered polybutadiene-diols (LCPBDs) with the comb-like architecture were prepared by radical reaction of a 5-(4-{[4-(octyloxy)phenyl]azo}-phenoxy)pentane-1-thiol with double bonds of telechelic HO-terminated polybutadiene (PBD); several polymers with various initial molar ratios of thiol to double bonds of PBD, R_0, in the range from 0 to 1 were prepared. DSC, polarizing microscopy, WAXS and dielectric relaxation spectroscopy (DRS) were employed to investigate their thermal and dielectric behavior in relation to morphology. DRS of the LCPBDs have revealed both collective and individual dynamic motions of molecules. Secondary β- and segmental α-relaxation were observed in unmodified PBD. In the LCPBDs, two secondary γ- and β- and two high-temperature α- and δ-relaxations were observed and assigned to specific molecular motions; all relaxations were analyzed and discussed in terms of time scale (Arrhenius diagram), magnitude (relaxation strength) and shape of the response.

Keywords: Liquid crystalline polybutadiene-diols; Dielectric spectroscopy; Mesophase transitions

1. Introduction

Introduction of rigid mesogenic groups into a polymer (backbone or side chains) usually leads to liquid crystalline polymers (LCP), which show an intermediate state of aggregation between the crystalline and the amorphous structures [1,2]. In liquid crystalline side chain polymers (LCSCPs) the mesogens are decoupled from the main chain by a spacer, which usually consists of aliphatic segments [3]. Generally, LC mesophase (showing a more ordered smectic or less ordered nematic structure) greatly affects physical properties of LCP. From polymers, processable films could be developed for photonic, ferroelectric and antiferroelectric applications and second harmonic generation in non-linear optics (NLO) [3,4]. Such systems, especially with azobenzene moieties in chains, have been extensively studied in recent years [5–8]. Azopolymers form a class of photochromic materials in which usually birefringence and optical dichroism, based on *cis*/*trans* photoisomerisation of azochromophores, can be initiated by polarized light since the transition dipole moment of azobenzene groups is oriented along the molecular axis of elongated *trans* isomer; dichroism and birefringence can be erased by subsequent irradiation with non-polarized light [9–11]. Stability of dichroism and birefringence depend on molecular motions in polymer. Optical and mechanical investigations were made on ordered polyurethane systems (LCPUs), based on diethanolamine derivatives with azobenzene grouping in side chain and diisocyanates of various flexibility [10–13]; such systems usually exhibit quite high values of the glass transition temperatures ($T_g \sim 90$ °C) and LC and crystalline transition temperatures (above 100 °C).

Recently [14] we have synthesized a new biphenyl-type of LC thiol which was used for preparation of comb-like LC polybutadiene-diols by radical addition of the thiol onto the

* Corresponding author. Faculty of Mathematics and Physics, Charles University, V Holešovičkách 2, 180 00 Prague 8, Czech Republic. Tel.: +420 221912363; fax: +420 221912350.
E-mail address: ilavsky@kmf.troja.mff.cuni.cz (M. Ilavský).

0032-3861/$ - see front matter © 2007 Elsevier Ltd. All rights reserved.
doi:10.1016/j.polymer.2007.07.032

double bonds of PBD; several LCPBDs with various initial molar ratios of thiols to double bonds of PBD, R_0, were made. Structural thermal transitions were investigated by DSC and dynamic mechanical spectroscopy. With increasing thiol content the glass transition temperature of LCPBDs, T_g, increases from ~−45 °C (neat PBD) to ~20 °C ($R_0 = 1$). LC transition starts at $R_0 = 0.3$ (the transition temperature $T_m \sim 27$ °C). With increasing R_0 temperature T_m increases and for $R_0 = 1$ reaches the value $T_m \sim 74$ °C; at the same time also the change in enthalpy at LC transition increases. It was found that the shape and position of mechanical functions on frequency (or temperature) scale and free-volume parameters determined from mechanical behavior strongly depend on degree of modification of PBD chains. This means that LCPBDs exhibit much lower T_g and T_m temperatures in comparison with LCPUs based on LC diethanolamine derivatives. In addition structural transitions of LCPBDs can be regulated by the amount of thiol bound to PBD chain.

Dielectric relaxation spectroscopy in broad frequency and temperature regions is one of the most effective tools for characterization of molecular motions in polymer systems [15] as various relaxation mechanisms can be expressed in terms of relaxation times and their temperature dependences, magnitude and shape of dielectric response. Dielectric spectroscopy of liquid crystalline side chain polymers (LCSCP) was pioneered by Kresse and coworkers. Zentel et al. developed a nomenclature for dielectric relaxation processes of LCSCP [16,17]. It was found that the dependences of dielectric functions on frequency and temperature are sensitive to the ordered state due to more or less aligned parts of macromolecules. Dielectric behavior in the LC state reflects a coupled response of ordered mesogenic groups to the applied electric field. The structure transitions detected by DSC are also observed by dielectric spectroscopy.

In this paper physical properties of a new comb-like LC polybutadiene-diols (LCPBDs) with azobenzene moieties in the side chain mesogens are described; LCPBDs were made by radical addition of 5-(4-{[4-(octyloxy)phenyl]azo}phenoxy)pentane-1-thiol onto the double bonds of PBD with various initial molar ratios of thiol to double bonds. Thermal structural transitions in LCPBDs are investigated by DSC, WAXS and polarizing microscopy; the broad-band dielectric spectroscopy is used for investigation of molecular dynamics in these LCPBDs. We believe that these systems, as well as linear polyurethanes and networks formed from LCPBDs, diisocyanates and triols, will find optical applications; in fact one LCPBD with $R_0 = 0.4$ was already used in optical investigations at room temperature and promising results were already submitted for publication [18].

2. Experimental

2.1. Preparation of LCPBDs

PBD: the telechelic OH-terminated polybutadiene diol − Krasol LBH 3000 (PBD) (Kaučuk Kralupy, $M_n \sim 2400$, 60 mol.% of 1,2 and 40 mol.% of 1,4 monomer units, number-average OH functionality $f_n = 2$) of the structure:

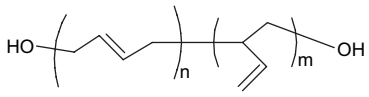

PBD

was purified by addition of silica gel Silpearl (Glass Works Kavalier). Silica gel was repeatedly washed with deionized water, then its stirred suspension was boiled in water for 3 min and silica gel was filtered off. It was placed in an oven and heated to 160–180 °C under nitrogen atmosphere for 24 h. After cooling to ambient temperature the activated silica gel was used to remove the antioxidant − Irganox 1520 from PBD; 20 g of PBD was dissolved in 100 ml of benzene (dried over Na) and 5 g of activated silica gel was added to the solution. The mixture was stirred under N_2 atmosphere for 6 h. Then SiO_2 was filtered off, solvent was removed on a rotavapor and PBD was dried to constant weight (50 °C/6.7 Pa).

LC thiol: the synthesis of LC thiol − 5(4-{[4-(octyloxy)-phenyl]azo}phenoxy)pentane-1-thiol (TH1) containing azobenzene mesogenic group of the structure:

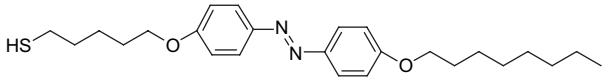

TH1

has proceeded in four steps: initial step was preparation of 4-(octyloxy)aniline by alkylation of 4-acetamidophenol and KOH mixture with octyl bromide. In the second step 4-hydroxy-4′-(octyloxy)azobenzene was synthesized by azocoupling of 4-(octyloxy)aniline with phenol. In the third step 4-[(5-bromopentyl)oxy]-4′-(octyloxy)azobenzene was prepared by the reaction of 4-hydroxy-4′-(octyloxy)azobenzene with 1,5-dibromopentane in dry acetone in the presence of K_2CO_3. Finally, thiuronium salt prepared from 4-[(5-bromopentyl)oxy]-4′-(octyloxy)azobenzene and thiourea was alkaline hydrolyzed yielding TH1. More details about TH1 synthesis can be found in Ref. [18]. TH1 was used in grafting reaction of the terminal thiol HS group with double bonds of PBD.

LCPBDs: in radical addition of TH1 onto double bonds of PBD 2,2′-azoisobutyronitrile (AIBN) was used as initiator. The reaction proceeded in toluene solution (54 g of PBD in 1 l of toluene) at the initiator-to-thiol ratio 5×10^{-2} mol at 60 °C for 48 h. We have synthesized LCPBDs with various initial molar ratios of thiols to double bonds of PBD, R_0, in the range from 0 to 1 (Table 1). The structure of LCPBDs is as follows:

Table 1
^{1}H NMR structure analysis of neat and modified LCPBDs

R_0	$D_{m(NMR)}.100$	HPB (mol.%)	PB (mol.%)	Pendant vinyl (mol.%)	*Trans* + *cis* (mol.%)
0	–	5.1	94.9	61.5	33.4
0.2	21.8	24.1	54.1	25.3	28.8
0.4	39.3	23.5	37.2	12.8	24.4
0.6	54.0	17.5	28.5	7.7	20.8
0.8	74.0	4.5	21.5	4.5	17.0
1.0	83.9	0	16.1	1.6	14.5

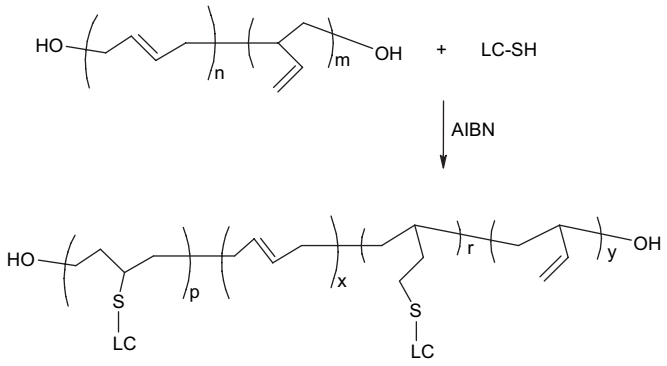

2.2. Characterization of LCPBDs

The degree of modification, D_m ([bound thiols]/[double bonds], mol/mol), after the addition and purification, was determined from elemental analysis using the relation:

$$D_{m(s)} = 32 \times w_s/(54 + 427.6 \times w_s) \quad (1)$$

where w_s is the weight fraction of sulfur bonded in LCPBDs as determined by elemental analysis.

The degrees of modification were determined also by ^1H and ^{13}C NMR spectroscopy (300.1 and 75 MHz, respectively, 60 °C). For $D_{m(NMR)}$ determination the integrated intensity of the signal of OCH_2 of LC-thiol protons at 4.0 ppm (or the signal of aromatic protons) was used. In this case the detailed structure of LCPBDs (amount of 1,2 and 1,4 butadiene units [19], hydrogenated PBD units and OH end groups [20]) could be evaluated.

The number- (M_n) and weight-average (M_w) molecular weights were determined by GPC (modular LC system with refractive index detection, column 30×8 SDV 10 000) calibrated with PS standards. THF was used as solvent and measurements were carried out at ambient temperature. From M_n, values the degrees of modification, $D_{m(GPC)}$ were determined.

2.3. Dielectric, DSC, WAXS and polarizing microscopy measurements

Dielectric measurements were carried out with a Schlumberger 1260 frequency-response analyzer with a Chelsea dielectric interface, in combination with the Quatro cryosystem of Novocontrol. The samples were pressed between brass electrodes 15 mm in diameter with a spacing of 55 μm, maintained by silica fibers. The dielectric permittivity $\varepsilon^*(f) = \varepsilon'(f) - i\varepsilon''(f)$ (f is frequency, ε' is the real (storage) and ε'' is the imaginary (loss) component, $i = \sqrt{-1}$) was measured in the frequency range 10^{-1}–10^6 Hz at temperatures between −150 and 130 °C upon heating (after cooling the sample to −150 °C from the isotropic state at 140 °C).

The frequency dependence of the complex dielectric function $\varepsilon^*(f)$ originates from fluctuations of molecular dipoles and/or dipoles induced by the charge separation at boundary layers inside the material (Maxwell–Wagner–Sillars polarization, MWS) or between the material and the electrodes (electrode polarization), and from the propagation of mobile charge carriers [11]. The frequency dependence of the dipole contribution to the complex dielectric function, ε_d^*, is usually described by the non-symmetrical Havriliak–Negami empirical equation [21]:

$$\varepsilon_d^* = \varepsilon_\infty + \Delta\varepsilon/[1 + i(f/f_r)^a]^b \quad (2)$$

with five generally temperature-dependent parameters: high-frequency (unrelaxed) value of the real part of permittivity ε_∞, the relaxation strength $\Delta\varepsilon = \varepsilon_0 - \varepsilon_\infty$ (ε_0 being the relaxed low-frequency value of permittivity), frequency f_r corresponding to the most probable relaxation time τ_r ($2\pi f_r \tau_r = 1$) and two shape parameters a and b. The parameter f_r is related to the peak frequency f_m at which the loss component ε'' attains its maximum value accounting to the following equation:

$$\left(\frac{f_m}{f_r}\right)^a = \frac{\sin\left(\frac{a\pi}{2(b+1)}\right)}{\sin\left(\frac{ab\pi}{2(b+1)}\right)} \quad (3)$$

In the case of symmetrical Cole–Cole distribution ($b = 1$), the frequencies f_r and f_m are identical [16]. A computer program based on the Marquardt procedure [22] was developed for determination of all parameters from the frequency dependence of ε'' at various temperatures.

The temperature dependence of frequency f_m could be described either by the Arrhenius equation:

$$f_m = f_\infty \exp(E_a/kT) \quad (4)$$

where E_a is the activation energy and f_∞ is the pre-exponential frequency factor, or by the Vogel–Fulcher–Tammann equation (VFT) [15,17]:

$$\log f_m = \log f_\infty - \frac{B}{T - T_0} \quad (5)$$

where B is the apparent activation energy, f_∞ the pre-exponential frequency factor, and T_0 the Vogel temperature ($T_0 \sim T_g - 50$ °C, where T_g is the glass transition temperature).

The frequency dependence of the conductivity contribution to the complex dielectric permittivity, ε_c^*, can be described by the following equation [17]:

$$\varepsilon_c^* = \left(i\frac{f}{f_0}\right)^\eta \quad (6)$$

where f_0 is an adjustable parameter and the exponent η would have the value -1 in the ideal case of pure time-independent dc conductivity.

The frequency dependence of the complex conductivity $\sigma^*(f)$ is given by the equation [17]:

$$\sigma^*(f) = i2\pi f \varepsilon_\circ \varepsilon^*(f) \quad (7)$$

and of the complex electric modulus $M^*(f)$ by:

$$M^*(f) = \frac{1}{\varepsilon^*(f)} \tag{8}$$

which is often used as alternative representation when emphasis is put on the charge carriers' transport.

Thermal properties were measured using a Perkin–Elmer differential scanning calorimeter DSC-7e. In order to avoid any thermal prehistory, samples were first heated to an isotropic melt, and reproducible data were collected on cooling and subsequent heating at a rate of 10 K/min (Fig. 2).

Wide-angle X-ray diffractograms were taken on a HZG4A diffractometer (Freiberger Präzisionsmechanik, Germany) using Ni-filtered Cu Kα radiation. For high-temperature measurements a heating chamber with thermal stability of 0.5 °C was attached.

The texture of crystalline and LC phases was determined by a polarizing optical microscope (Nicon Eclipse 80i, crossed polarizer's) equipped with a heating stage. The heating/cooling rate was 3 K/min.

3. Results and discussion

3.1. Modification of LCPBDs

Detailed structure of neat PBD and modified LCPBDs (amount of 1,2 and 1,4 butadiene units, hydrogenated PBD units and OH end groups) evaluated from ^{1}H NMR spectroscopic measurements is shown in Table 1. It can be seen that with increasing initial molar ratio of thiol to double bonds of PBD, R_0, the fraction of grafted PBD monomer units increases; in addition, some amount of hydrogenated units (HPB) in LCPBDs is formed. While for unmodified PBD ($R_0 = 0$) fraction of HPB is ~0.05, after modification, the highest obtained value of HPB ~0.24 was for $R_0 = 0.2$; further increase in R_0 leads to a decrease in HPB and for $R_0 = 1.0$ fraction of HPB is 0. It is interesting to note that at the highest modifications practically all pendant (1,2) double bonds were consumed while a substantial amount of backbone (1,4) double bonds remained. This suggests that the SH groups of thiol preferably reacts with pendant double bonds of PBD. This finding is in agreement with previous results obtained on model reaction of thiyl radical which attacks the double bond of alkene; it was found that the reactivities of thiol with 1- and 2-alkenes differ [23]. ^{1}H and ^{13}C NMR spectroscopies have also proved that the OH functionality of LCPBDs does not change with the extent of the addition reaction.

Comparison of various experimental degrees of modification, D_m, obtained from GPC, $D_{m(GPC)}$, (from number-average molecular weights M_n), sulfur content, $D_{m(S)}$, and ^{1}H NMR analysis, $D_{m(NMR)}$ in dependence on initial ratio R_0 is shown in Fig. 1. As expected, modification degrees D_m, determined by all three methods, increase with increasing initial ratio R_0. While for the lowest initial thiol ratios R_0 ($R_0 \leq 0.4$), $R_0 \sim D_m$, for higher R_0, $D_m < R_0$ were found. Lower D_m values suggest that at the higher R_0 values steric hindrance

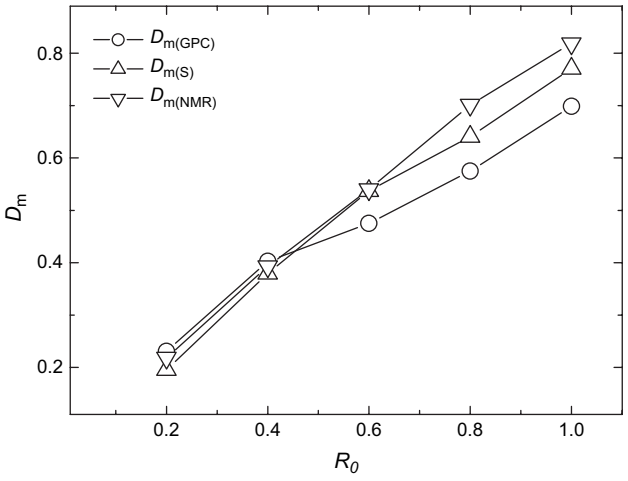

Fig. 1. Determined degrees of modification D_m (from S content – $D_{m(S)}$, from GPC – $D_{m(GPC)}$ and from ^{1}H NMR – $D_{m(NMR)}$) in dependence on initial ratio of thiol/double bonds – R_0.

probably prevents the addition reaction and thiol is subsequently removed from polymer during purification. We believe that also dimerization of thiols can take place in the presence of initiator by recombination of thiol radicals; the lowest $D_{m(GPC)}$ values suggest that some of these dimmers remain in the modified PBD even after purification.

3.2. Thermal behavior of unmodified PBD, thiol and LCPBDs

An example of measured DSC traces of neat thiol and LCPBD with $R_0 = 1.0$ is shown in Fig. 2; the corresponding transition temperatures (the glass transition – T_g and melting temperatures – T_{mi}) determined from DSC thermograms in cooling (C) and subsequent heating (H) scans are summarized in Table 2. Wide-angle X-ray diffraction (WAXS) data for thiol and LCPBD with $R_0 = 1.0$ are shown in Fig. 3. From Table 2 it follows that on cooling of the thiol first mesophase formation takes place at ~116 °C ($\Delta H_m \sim -4.6$ J/g, SmA phase in which the centers of mass of the rods are in one dimensional periodic order parallel to long axes of the rods); next transition is at 100 °C ($\Delta H_m \sim -2.6$ J/g, SmC phase with tilted molecules to long axes). Two smectic phases have been usually found in the case where azobenzene grouping is present in organic LC molecules with flexible spacer [24,25]. WAXS measurements (Fig. 3) showed that at 95 and 77 °C diffractograms of thiol consist of one strong, narrow reflection the position of which corresponds to 3.04 nm and a broad amorphous halo. Theoretical atomistic simulations of thiol using software BIOSYM led to the length of ~3.2 nm, which agrees well with the found one. Due to this we assume that a smectic structures exist in thiol; this periodicity stays in crystalline phase at lower temperatures. The crystallization of TH1 on cooling takes place at ~60 °C ($\Delta H_m \sim -17.7$ J/g). From WAXS measurements periodicities of 3.12 and 1.88 nm were determined at 70 °C; the amorphous profile is overlapped by several narrow reflections, which indicate a lateral order of thiol chains

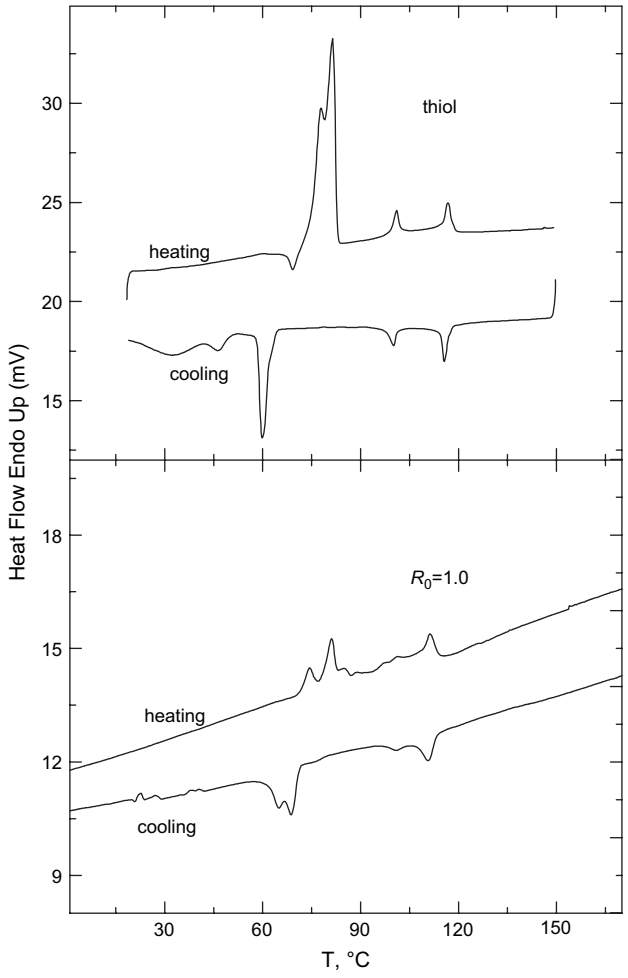

Fig. 2. Example of measured DSC traces for neat thiol and LCPBDs with $R_0 = 1.0$. Cooling and heating rate was 10 K/min.

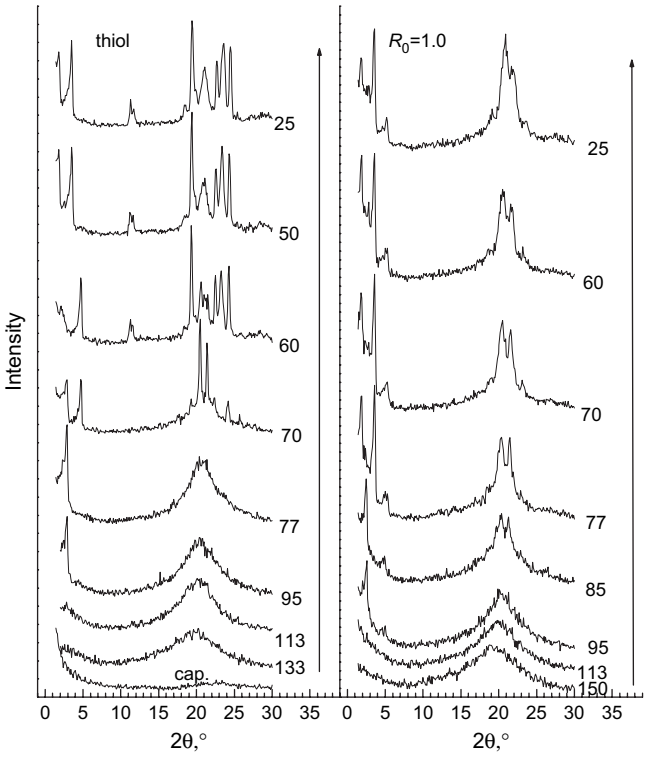

Fig. 3. X-ray scattering diffractograms for thiol and LCPBD with $R_0 = 1.0$ obtained on cooling. The numbers at curves denote temperatures in °C.

(especially of the mesogenic groups). As follows from Fig. 2 two transitions associated with reorganization of crystal phase have appeared at ~45 and 32 °C (sum of both $\Delta H_m \sim -18.3$ J/g and denoted as T_{m1} in Table 2); periodicities of 4.9 and 2.52 nm were found at 60 °C from WAXS (Fig. 3). On subsequent heating, small recrystallization (Fig. 2) followed by melting of the crystalline phase at temperature ~81 °C ($\Delta H_m \sim 61$ J/g) was observed (Table 2). At temperatures higher than 85 °C, a SmC structure appears; this structure melts at 101 °C ($\Delta H_m \sim 2.7$ J/g) to SmA mesophase which finally melts to an isotropic state at 117 °C ($\Delta H_m \sim 3.2$ J/g, Table 2).

From DSC traces of LCPBD with $R_0 = 1.0$ shown in Fig. 2 it follows that modification leads to simpler thermal behavior in comparison with neat thiol (see also Figs. 3 and 4). On cooling only one mesophase seems to be formed at ~111 °C ($\Delta H_m \sim -8.2$ J/g, Table 2); crystallization starts at ~75 °C ($\Delta H_m \sim -12.4$ J/g) and final structure formation takes place at ~65 °C ($\Delta H_m \sim -5.9$ J/g, Table 2). On heating crystalline structure melts at ~75 °C ($\Delta H_m \sim 3.7$ J/g) and ~81 °C

Table 2
Degree of modifications and DSC transitions of thiol, PBD and LCPBDs

R_0	$D_{m(S)}$	Run	T_g (°C)	Δc_p (J/g K)	T_{m1} (°C)	ΔH_{m1} (J/g)	T_{m2} (°C)	ΔH_{m2} (J/g)	T_{m3} (°C)	ΔH_{m3} (J/g)	T_{m4} (°C)	ΔH_{m4} (J/g)
Thiol	0	H					81.4	60.8	100.9	2.7	116.9	3.2
		C			32.4	−18.3	59.9	−17.7	100.0	−2.6	115.6	−4.6
PBD	0	H	−47.3	0.49								
		C	−44.2	0.42								
0.2	0.195	H	−15.9	0.15	−8.3	1.3	54.8	5.2	89.5	0.8		
		C	−12.5	0.29			41.2	−3.1	80.2	−0.5		
0.4	0.379	H			−7.2	1.8	54.6	7.5	84.5	7.0		
		C			−4.7	−4.8			79.3	−3.3		
0.6	0.537	H					72.9	5.60			103.1	6.1
		C					60.2	−1.32			102.7	−9.7
0.8	0.641	H					73.1	11.8	85.6	3.8	105.1	8.9
		C					62.1	−8.7	74.7	−1.7	108.2	−9.5
1.0	0.771	H					74.7	3.7	81.2	11.4	111.3	7.1
		C					64.5	−5.9	74.5	−12.4	110.9	−8.2

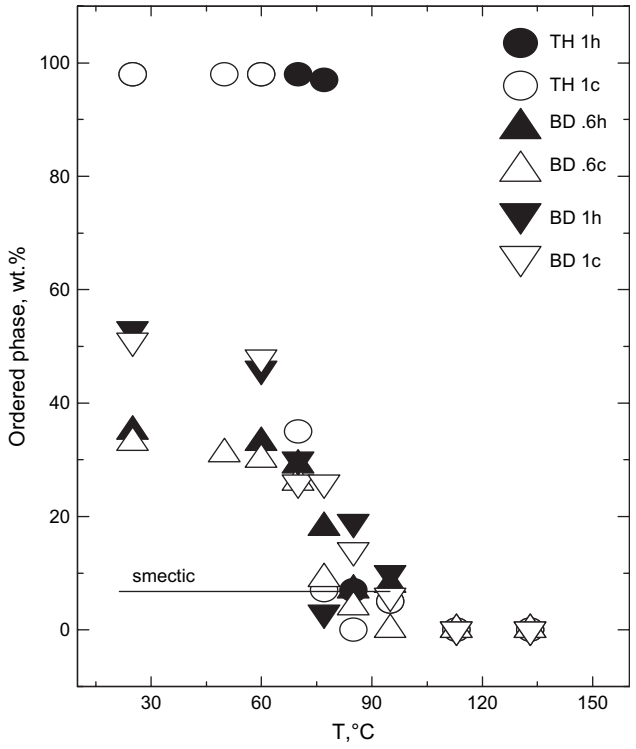

Fig. 4. Temperature dependence of the weight fractions of the ordered phase determined on cooling (open symbols) and subsequent heating (full symbols) for thiol and LCPBD with $R_0 = 0.6$ (BD.6) and $R_0 = 1.0$ (BD1).

($\Delta H_m \sim 11.4$ J/g) to smectic mesophase which melts at ~ 111 °C ($\Delta H_m \sim 7$ J/g). As expected, lower ΔH_m values were found for modified LCPBDs in comparison with those of neat thiol (Table 2). The T_g transition could be observed on DSC thermograms only for LCPBD with $R_0 = 0.2$; higher modifications exhibit only crystal/mesophase/isotropic state transition (it is in agreement with dielectric results shown in Fig. 10). As T_g for LCPBD with $R_0 = 0.2$ has increased for about 30 °C we believe that for LCPBDs with $R_0 > 0.2$ the values of T_g have increased into temperature region of ordered phases formation.

From the WAXS patterns of LCPBD with $R_0 = 1.0$ (Fig. 3), it can be seen that on cooling the smectic structure in polymer is formed at 95 °C with the periodicities of ~ 3.39 and 1.7 nm (the first value agrees well with the length of the thiol molecule). At 85 °C the crystallization starts and the amorphous profile is overlapped by reflections indicating lateral order of grafted chains. At 77 °C lamellar periodicities of 4.72, 2.45 and 1.7 nm, which reflect mutual ordering of grafted side chains, were determined. Below 77 °C the same structure remains. On subsequent heating the diffractograms revealed a structure change from crystalline to LC smectic texture at 85 °C and at 95 °C; the same periodicities were determined as in the cooling regime (3.39 and 1.7 nm). Further heating above 115 °C melts the sample, and the diffractograms correspond to a completely amorphous structure of the polymer. Comparison of WAXS patterns of the thiol and LCPBD with $R_0 = 1.0$ reveals that even though in both samples similar ordered structures were formed (Fig. 3), in thiol at the low temperatures better organized and more extensive crystalline structure was developed. This is in agreement with Fig. 4 in which the temperature dependences of weight fractions of the ordered phase determined from X-ray diffractograms (from area below peaks) are shown. While almost all thiol is involved in the crystalline phase (98–95 wt.%) at the lowest temperatures, only ~ 33 and ~ 52 wt.% of sample is involved in the crystalline structure for LCPBDs with $R_0 = 0.6$ and 1.0, respectively. These results are also confirmed by polarizing microscopy measurements shown in Fig. 5; a better developed ordered smectic and crystalline structure can be seen for thiol than for sample with $R_0 = 1.0$.

As expected, simple amorphous behavior with only the glass transition temperature T_g was found for PBD; the change in the specific heat $\Delta C_p \sim 0.45$ J/g K shows a value typical of amorphous polymers (Table 2) [26]. The same results for unmodified PBD of similar microstructure were obtained earlier by Hofmann et al. [27].

3.3. Dielectric behavior of unmodified PBD, thiol and LCPBDs

It is well known that all glass-forming polymers exhibit primary relaxation – α; this relaxation is assigned to motion of polymer main chain segments and is related to the glass transition (dynamic glass transition). The temperature dependence of its relaxation time is described by the Vogel–Fulcher–Tammann (VFT) Eq. (5), which describes the slowing down of the relaxation approaching to the glass transition temperature. Besides the α-relaxation, usually additional (secondary) relaxations (β- or γ-relaxations) of faster time scales take place at lower temperatures. The β- and γ-processes generally occur in the glassy state, and have different molecular nature compared with the α-relaxation [17]. These secondary relaxations usually exhibit an Arrhenius temperature dependence of relaxation times (Eq. (4)), in contrast to the much stronger VFT temperature dependence found for primary α-relaxation.

The overall dynamics in side chain liquid crystalline polymers is characterized by four dielectric relaxation processes, γ, β, α and δ, in the order of increasing temperature or decreasing frequency. The γ process is related to rotational fluctuations of the terminal groups of the side chain, the β-relaxation corresponds to liberation fluctuations of mesogens around the long molecular axis and the α-relaxation is assigned to fluctuations of segments of the polymer main chain as they are observed in glass-forming systems. The δ-relaxation is assigned to liberation fluctuations of mesogens around the short molecular axis; presumably it is a rather multistep process with motional averaging rather than a 180 flip-flop jump of the mesogens [16,17].

3.3.1. Temperature dependences of dielectric behavior

Fig. 6 displays the temperature dependence of the real (a) and the imaginary (b) part of the complex dielectric permittivity at a fixed frequency of 500 Hz measured for the unmodified PBD and all the LCPBDs (isochronal plot). Dielectric data were measured isothermally, upon heating from the solid state,

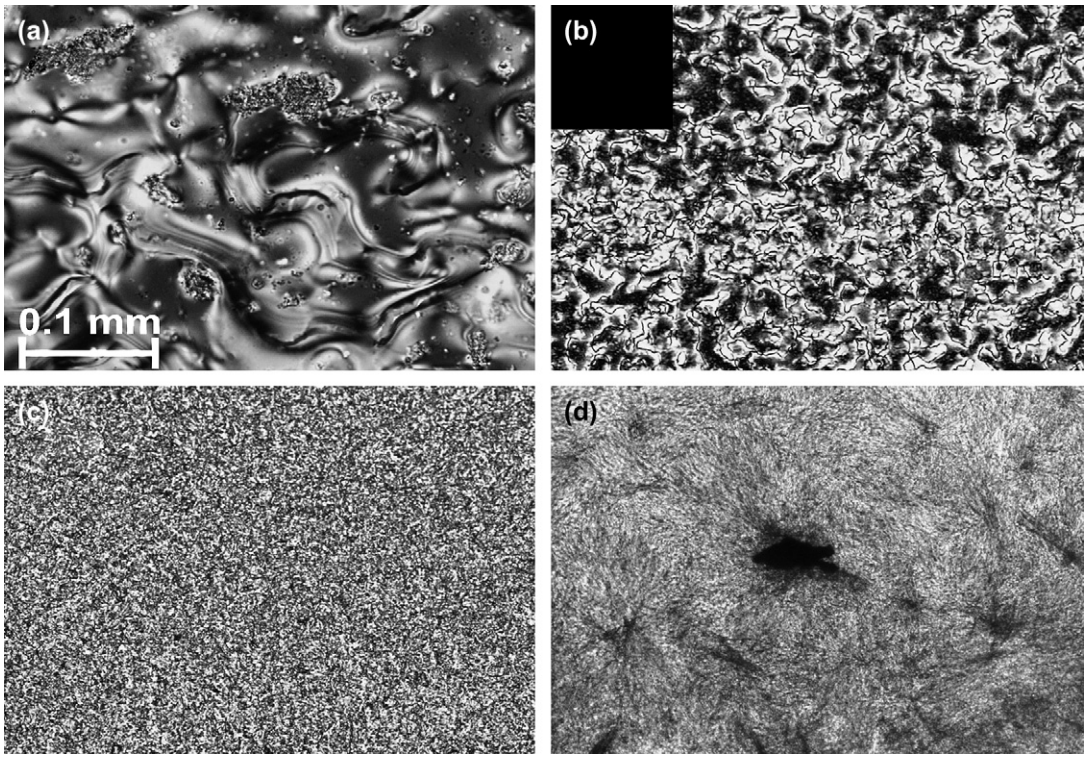

Fig. 5. Optical micrographs of thiol (a, c) and LCPBD with $R_0 = 1$ (b, d): a – thiol 95 °C, b – LCPBD 95 °C, c – thiol 25 °C, d – LCPBD 25 °C.

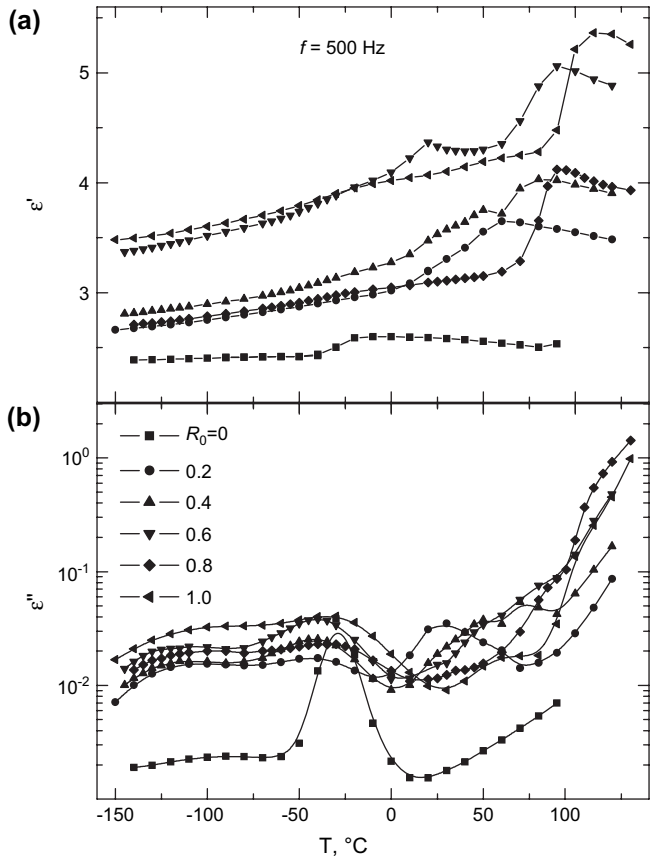

Fig. 6. Temperature dependence of dielectric storage, ε' (a) and dielectric loss, ε'' (b) component measured at 500 Hz for unmodified PBD and LCPBDs.

as a function of frequency and represented as a function of temperature at a constant frequency; this plot allows to follow the overall dielectric behavior of the materials under study. In such representation contribution from each relaxation process is observed as a stepwise increase with increasing temperature, in the real part ε' and as a peak in the imaginary part ε''. The change in molecular mobility, when passing from the crystalline state (where small-scale motions can take place) to the intermediate liquid crystalline state (where collective motions may occur), can be followed as a significant increase in ε' with increasing temperature. Transition from the ordered to the isotropic liquid state is indicated by a decrease in ε' with increasing temperature as a result of the thermal motion which disturbs the orientation of molecular dipoles.

In unmodified PBD two processes are observed as peaks in ε'' at ~ -30 °C and the small one at ~ -90 °C for the selected frequency (500 Hz), can be observed (Fig. 6). The relaxations are assigned to the local motion of pendant vinyl groups (β-relaxation) and to the segmental motion of the main polymer chain (α-relaxation), respectively. The decrease in ε' at high temperatures (>100 °C) is due to the thermal motion, which does not allow the orientation of the dipoles.

For LCPBDs, higher values of ε' are detected as compared with that of the unmodified PBD indicating a higher molecular mobility in the LCPBDs. This is due to incorporation of the thiol chains with polar groups into the PBD structure. The dependence of ε' on the R_0 is not linear, the polymers with high R_0 (0.6 and 1.0) are characterized by higher molecular mobility compared with those with lower R_0 (0.2 and 0.4). However, the maximum polarization increases nearly linear with the R_0

content (with the exception of the sample with R_0 equal to 0.8) due to an increase in the amount of polar groups with increasing R_0.

At low temperatures, in the solid state, two processes take place in all the LCPBDs, observed as peaks in ε'' at ~ -40 and ~ -110 °C. We believe that these relaxations can be attributed, in the order of increasing temperature, to the local motion of the octyloxy end groups of the side chain (γ-relaxation), and to the motion of the azobenzene moiety of the side chain around its long molecular axis (β-relaxation) without involving the motion of the side chains as a whole.

A significant change in ε' is observed (for the selected frequency) at temperatures above 0 °C for the LCPBDs with R_0 equal to 0.2 and 0.4. For the LCPBDs with R_0 equal to 0.6, 0.8 and 1.0, this change is observed at temperatures above 50 °C. This change indicates a significant change in the molecular mobility of the polymers above the temperatures mentioned above, which correlates with the melting temperatures found by DSC measurements (Table 2).

A further increase in the temperature (above 90 °C) results in a decrease in ε' as a result of molecular thermal motion, which does not allow the orientation of the dipoles; the finding indicates the transition of the materials to the isotropic state. This means that at temperatures higher than the temperature at which the temperature coefficient of ε' changes from positive to negative, the materials are in the liquid state. The temperature at which transition to the isotropic state occurs increases with increasing R_0 and is in good agreement with the clearing temperatures found by polarizing microscopy and DSC measurements (Table 2). In the liquid crystalline state, the picture of the relaxation processes is complex, consisting of one or two peaks while in the isotropic state only dc conductivity maintains (a steep increase in ε'' with increasing temperature).

3.3.2. Frequency dependencies of dielectric behavior

Fig. 7 displays the frequency dependences of the imaginary part of the dielectric permittivity, ε'', for the unmodified PBD in the temperature range between −35 and 5 °C. A well-resolved peak, which shifts to higher frequencies with increasing temperature, can be observed. This peak corresponds to the main relaxation (α), which is associated with the cooperative motion of segments of PBD backbone chains and is related to its glass transition.

As an example of the measured frequency dependences of the dielectric losses in the LCPBDs, data for the material with R_0 equal to 0.2 at several temperatures in the crystalline (a) and liquid crystalline (b) state are presented in Fig. 8. Two dielectric dispersions are observed in the crystalline state. The γ-relaxation is observed at very low temperatures as a broad peak which shifts to higher frequencies with increasing temperature. The γ-relaxation peak is followed by a narrower β-relaxation peak detectable in the frequency window of dielectric measurements in the temperature range between −50 and 0 °C. The same relaxations are observed for all the LCPBDs, a detailed analysis and discussion of them follows. The assignment of these relaxations to particular molecular motions has been done in the previous subsection.

At high temperatures two dispersions are also observed (Fig. 8b). The faster relaxation, observed as a shoulder on ε'' vs. f dependences, shifts from 100 Hz at 20 °C to 100 kHz at 60 °C, while the slower relaxation is observed as a change in the slope of ε'' vs. f at low frequencies. The faster relaxation

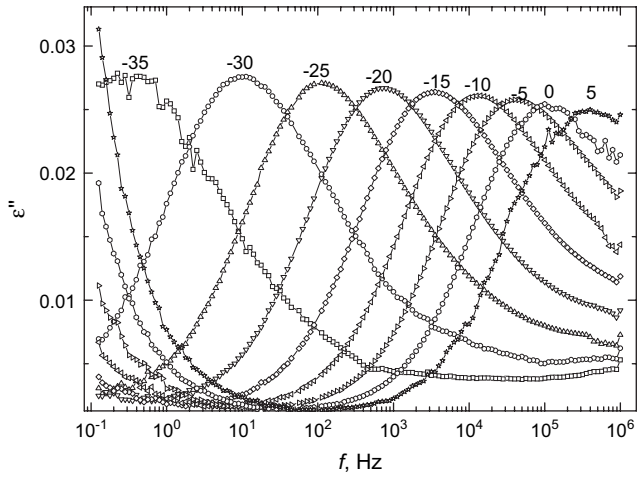

Fig. 7. Frequency dependence of dielectric loss, ε'', for PBD in the region of the main α-relaxation. The numbers at curves denote temperatures in °C.

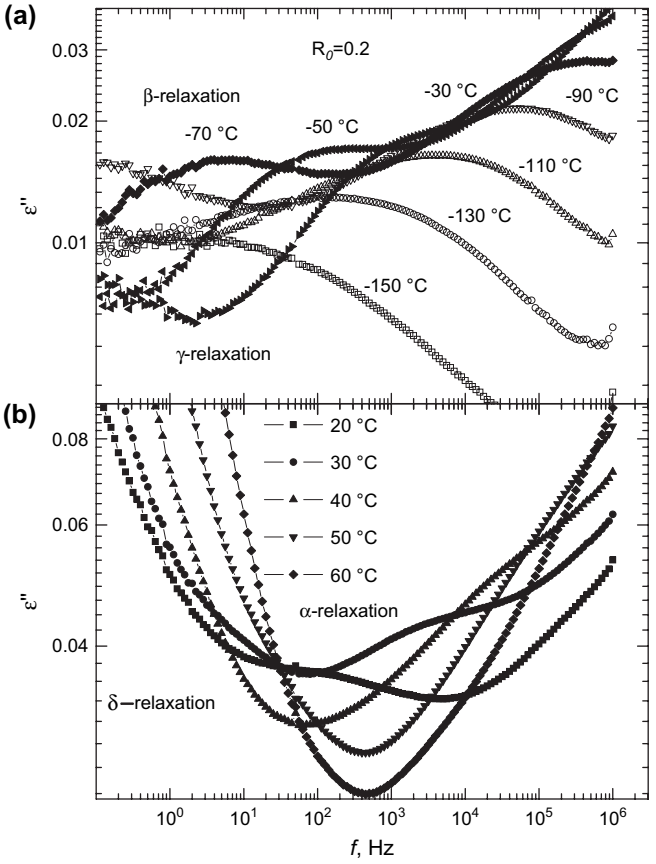

Fig. 8. Dielectric loss component ε'' as a function of frequency for the LCPBD with $R_0 = 0.2$ at low (γ- and β-relaxation (a)) and high (α- and δ-relaxations (b)) temperatures.

is attributed to α-relaxation, which is associated in liquid crystalline polymers with reorientations of the polymer backbone and spacer, while the slower relaxation is attributed to the δ-relaxation. The α-relaxation is observed only for the polymer with $R_0 = 0.2$, while the δ-relaxation is observed as a well-resolved peak for the materials with $R_0 = 0.4$, 0.6 and 0.8. The increase in ε'' with decreasing frequency observed at low frequencies in Fig. 8b originates from the propagation of mobile charge carriers (conductivity contribution) [17].

In order to extract quantitative information on the time scale, as well as on the strength and shape of the observed dielectric relaxations, the decomposition procedure for fitting the data was used. In principle, the HN function (Eq. (2)) is used for the description of frequency dependences of an individual relaxation process. This method works well when all processes are reasonably separated, as in the case of the α-relaxation in the PBD. When they start to overlap (as in the case of relaxation processes in LCPBDs), the fitting procedure is getting difficult (e.g., HN parameters, which determine the high frequency part of the β-relaxation, and those which characterize the low-frequency part of the γ-relaxation affect each other [17]). Because of the problem mentioned above we assumed that all relaxations observed in the LCPBDs are well described by the simpler Cole–Cole distribution function, which results from the HN function with the b parameter equal to 1. The fitting procedure was based mainly on the frequency dependences of the imaginary part of dielectric permittivity ε''.

An example of the fitting procedure is presented in Fig. 9 for the material with $R_0 = 0.6$ for the γ-, β- and δ-relaxations in the order of increasing temperature. The sharp increase in dielectric losses with decreasing frequency observed at the highest temperature corresponds to the conductivity contribution and was fitted by adding the term given in Eq. (6) to the Cole–Cole function used for the δ-relaxation. Two dielectric dispersion regions (γ and β) could be determined from the data measured at −50 °C, while for the lowest presented temperature (−125 °C) only a single process (γ-relaxation) is observed. In some the cases' information was extracted from the temperature dependence of ε'' at a fixed frequency (isochronal plot). The results of the above analysis for each relaxation observed in the PBD and the LCPBDs, can be summarized as follows.

3.3.2.1. Unmodified PBD

3.3.2.1.1. α-Relaxation. The α-relaxation peak is well described by the HN equation with mean values (with respect to temperature) of the shape parameters a and b equal to 0.7 and 0.4, respectively, indicating a relatively narrow and unsymmetrical peak with a slope on the low-frequency side higher than that on the side of high frequencies. The relaxation strength $\Delta\varepsilon$ was found to be nearly temperature-independent, with a mean value equal to 0.14, which is reasonable because of the nonpolar character of polybutadiene. The temperature dependence of the peak frequency f_m of the α-relaxation is well described by the VFT equation with parameters $f_\infty = 10^{11}$ Hz, $B = 1409$ K and $T_0 = 127$ K (Fig. 10, full squares). The glass transition temperature obtained from the dielectric data as the temperature at which the relaxation time is equal to 100 s [17], known as $T_{g,diel}$ which is equal to −42 °C (obtained by extrapolation of the VFT fitting curve to low frequencies) correlates well with the glass transition temperature measured by calorimetric measurements (Table 2). The glass transition temperature is in agreement with that reported in the literature for polybutadiene with the same fraction of pendant vinyl and linear butadiene units [28].

3.3.2.1.2. β-Relaxation. The β-relaxation can be followed only in the isochronal plot. The temperature dependence of the β-relaxation time, shown in Fig. 10 (full squares), follows the Arrhenius behavior, which is consistent with the origin of the relaxation. The values of activation energy E_a (0.43 eV) and pre-exponential frequency factor f_∞ (10^{15} Hz), calculated by linear fit to the data of the logarithm of peak frequency vs. $1/T$ (Eq. (4)), indicates a local process.

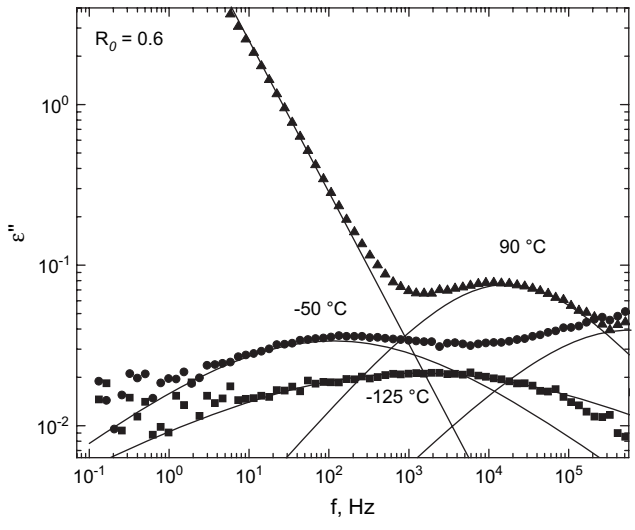

Fig. 9. An example of decomposition of ε'' vs. f dependences measured at indicated temperature for LCPBD with $R_0 = 0.6$.

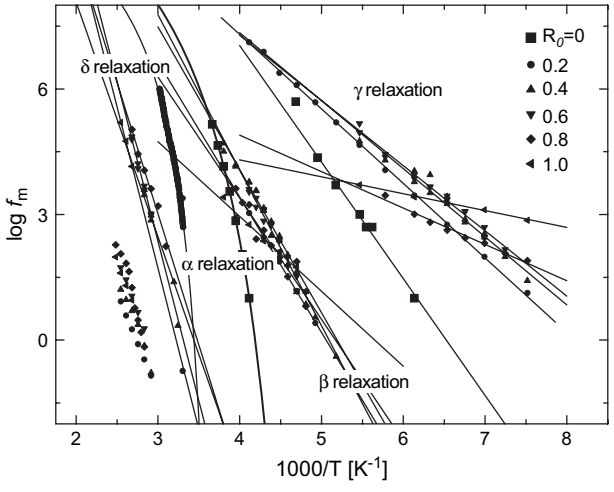

Fig. 10. Logarithm of the peak frequencies f_m as a function of inverse temperature for all the observed relaxations in PBD and LCPBDs (Arrhenius diagram). The lines are fittings of the dielectric data to the VFT or Arrhenius equation (depending on the relaxation process).

3.3.2.2. LCPBDs

3.3.2.2.1. γ-Relaxation. The strength of the γ-relaxation was found to increase slightly with increasing temperature, with the shape parameter a between 0.17 and 0.20, for all the materials without any specific dependence on composition. The relaxation becomes narrower as the temperature increases as it is expected for local relaxations; this reflects the homogenization of the environment of relaxing unit with increasing temperature. The mean value of the b parameter of the HN equation varies between 0.25 and 0.30 indicating a very broad relaxation. In the γ-relaxation peak also the β-relaxation of PBD can contribute due to a similar relaxation time of the two processes. However, the contribution of the β-relaxation is expected to be less with increasing R_0 value, due to a decrease in the vinyl group content (Table 1).

The temperature dependence of the peak frequency f_m of the γ-relaxation can be described by the Arrhenius equation (Fig. 10). The parameters of the Arrhenius equation (activation energy E_a and pre-exponential factor f_0) are listed in Table 3 for all the materials. The values of E_a and f_∞ indicate a locally activated process. Extraordinary low values for both parameters are calculated for the materials with high contents of side chains ($R_0 = 0.8$ and 1.0).

3.3.2.2.2. β-Relaxation. The strength $\Delta\varepsilon$ of the β-relaxation does not depend on temperature while it increases with increasing R_0, with the exception of the polymer with $R_0 = 0.8$, which in general is characterized by very low values of dielectric permittivity indicating a material with suppressed molecular mobility. The strength of the relaxation $\Delta\varepsilon$ ranges from 0.1, for the material with $R_0 = 0.2$–0.3 for the sample with $R_0 = 1.0$. This result is consistent with the interpretation given for this relaxation: with increasing R_0 the content of polar groups, which contribute to the β-relaxation, increases. The shape of the relaxation remains unchanged with temperature and it is almost independent of composition, while the value of α-parameter of HN was found equal to 0.4 for all samples. The temperature dependence of the peak frequency is well described by the Arrhenius equation (Fig. 10). For both activation parameters (E_a, f_∞) extraordinary high values are obtained (Table 3). Similar high values of E_a and f_∞ have been reported in the literature for side chain liquid crystalline polymers with the polar azobenzene moieties in side chains [29]. It was argued that this relaxation is associated not only with local motion of the mesogen in the potential formed by the surrounding molecules. Instead, it was suggested that neighboring molecules are involved as well in the liberation dynamics of the β-relaxation. The values of E_a and f_∞ were found to increase with increasing R_0, except for the materials with $R_0 = 0.8$ and 1.0.

3.3.2.2.3. α-Relaxation. The α-relaxation was observed only for the composition with the lowest $R_0 = 0.2$; this finding corresponds to DSC data (Table 2). The relaxation is observed as a peak in isothermal measurements of dielectric losses only at three temperatures in the frequency window of dielectric measurements. On the other hand, it can be followed in isochronal plots of dielectric losses as a peak which shifts to higher temperatures with increasing frequency. Because of the limited data for this relaxation from the isothermal data (the fitting was possible only for three temperatures), the information was extracted from the isochronal plots. The α-relaxation in the LCPBD with $R_0 = 0.2$ is observed at higher temperatures or lower frequencies as compared with that in unmodified PBD, indicating an increase in the glass transition temperature in LCPBDs. The maximum of the dielectric losses increases insignificantly, which is unexpected as in this type of relaxation, motion of segments with higher dipole moments is involved. The results can be understood in terms of an increase in stiffness of the main chain due to the interaction of pendant vinyl butadiene units with the SC units (strongly interacting), as was found by ^{1}H NMR measurements, resulting in a reduced segmental mobility. At high temperatures the relaxation rate follows the Arrhenius behavior, with extraordinary high values of activation energy and pre-exponential frequency factor (2.0 eV and 10^{38} Hz), which turns to a VTF-like dependence at a temperature, indicating a change in the molecular dynamics of the system (Fig. 10). Fitting of the data to VTF equation gives for the parameters of the equation, f_∞, B and T_0, the values 10^{11} Hz, 808 and 258 K, respectively.

The temperature at which the change of molecular dynamics occurs agrees with a phase transition temperature of the system – melting of crystalline phase as detected by DSC measurements. Finally, the maximum of dielectric losses as recorded from the isochronal plots was found to increase with increasing temperature. It can be assumed that this relaxation is suppressed in materials with higher R_0 as a result of the higher content of the ordered phase in samples.

3.3.2.2.4. δ-Relaxation. Information about the δ-relaxation is limited for some polymers; it can be extracted for few temperatures. The fitting procedure found the δ-relaxation only for the materials with $R_0 = 0.4$, 0.6 and 0.8. From the limited data for the shape parameter, a, and the intensity, $\Delta\varepsilon$, of the δ-relaxation, it can be concluded that the relaxation is narrow with an a parameter which ranges from 0.5 for the sample with $R_0 = 0.4$–0.7 for that with $R_0 = 0.8$. The strength of the relaxation $\Delta\varepsilon$ is 0.2 and 0.5 for the materials with $R_0 = 0.4$ and 0.6, respectively. For the sample with $R_0 = 0.8$, a lower value of $\Delta\varepsilon$ was found. The maximum of dielectric losses decreases with increasing temperature in the smectic phase and levels off in the isotropic state. The limited temperature data for this relaxation does not allow to conclude on the temperature dependence of its peak frequency f_m (Arrhenius or VFT behavior) (Fig. 10). Assuming the Arrhenius behavior, extraordinarily high values were calculated for the E_a and f_∞

Table 3
Parameters of Arrhenius equation for the dielectric relaxations of LCPBDs

[Thiol]/[PBD]	γ-Relaxation		β-Relaxation		δ-Relaxation	
R_0 mol/mol	f_∞ (Hz)	E_a (eV)	f_∞ (Hz)	E_a (eV)	f_∞ (Hz)	E_a (eV)
0.2	3×10^{14}	0.35	2×10^{16}	0.64	–	–
0.4	6×10^{13}	0.32	5×10^{17}	0.68	1×10^{19}	1.1
0.6	3×10^{13}	0.31	1×10^{19}	0.74	1×10^{25}	1.5
0.8	2×10^{8}	0.17	1×10^{15}	0.57	1×10^{22}	1.2
1.0	1×10^{6}	0.08	1×10^{10}	0.35	1×10^{25}	1.5

(Table 3), indicating a cooperative process. The cooperative character of this relaxation has been discussed in the literature [30]. In the smectic A phase this process is interpreted as being due to the side group flipping around the polymer backbone as the mesogen is hopping from one smectic layer to another [31]. This interpretation agrees well with the fact that in isotropic phase no such relaxation is observed, while the absence of this process in the material with $R_0 = 0.2$ may reflect the lower order within this sample as a result of the low side group content.

3.3.2.2.5. Conductivity. The information about the conductivity observed at high temperatures was extracted by analyzing the imaginary part of the complex electric modulus M'' in dependence on frequency (Eq. (8), Fig. 11). Representation of the data using the electric modulus formalism allows the observation of the conductivity as a peak on f, which is more convenient for analysis. As an example of the dependences of conductivity σ and electric modulus M'' as a function of frequency in a high temperature range related with conductivity phenomena for the material with $R_0 = 0.8$ is demonstrated in Fig. 11. A significant increase in conductivity is observed in the temperature range 95–105 °C, as compared with the increase in conductivity with temperature at temperatures below 95 °C and above 105 °C, indicating a change of the charge carrier mobility. The temperatures are in good agreement with the transition temperatures obtained by DSC measurements of these samples (Table 2). In the frequency dependence of the imaginary part of M'', a peak at 80–90 °C with a double structure can be observed, which narrows with no indication of double structure at higher temperatures. The relaxation observed as a shoulder at the high frequency side corresponds to relaxation of interfacial character of the Maxwell–Wagner–Sillars (MWS) type polarization as a result of the existence of layers with different conductivity within the material, while the peak at low frequencies corresponds to the conductivity relaxation due to the transport of mobile charge carriers. MWS polarization is observed also in the materials with $R_0 = 0.6$ and 0.8, indicating electrically heterogeneous materials due to the formation of the ordered smectic phase. Fig. 12 displays the frequency dependences of M'' and σ for all the materials at 120 °C (isotropic state). The materials can be classified into two groups; materials with $R_0 = 0.2$ and 0.4 and materials with $R_0 = 0.6$, 0.8 and 1.0, which differ in conductivity values by an order of magnitude and in peak frequency by one decade (peak shifts to higher frequencies with increasing conductivity).

The temperature dependence of the main peak frequency f_{max} (determined from the M'' vs. f dependences) can be described by the Arrhenius equation (Fig. 13). For the materials with $R_0 = 0.4$ and 0.8, significant changes in the relaxation rate, passing from the smectic to the isotropic state is observed, indicating a change of the mobility of the charge carriers in the two phases. For the material with $R_0 = 0.4$, the

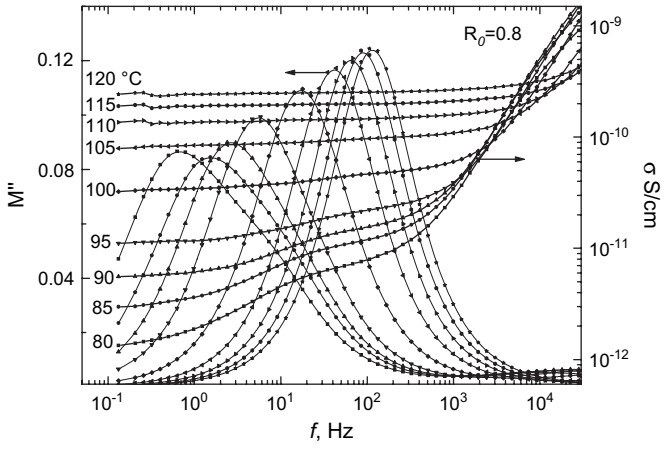

Fig. 11. Frequency dependence of the imaginary part of the complex electric modulus, M'' (left axis) and of the real part of complex conductivity, σ (right axis), for the LCPBD with $R_0 = 0.8$ at high temperatures, indicated on the plot.

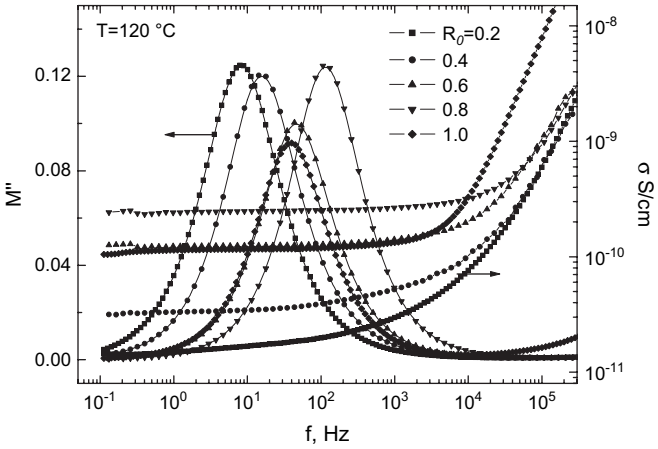

Fig. 12. Frequency dependence of the imaginary part of the complex electric modulus, M'' (left axis) and of the real part of complex conductivity, σ (right axis), for all the LCPBDs at 120 °C (isotropic state).

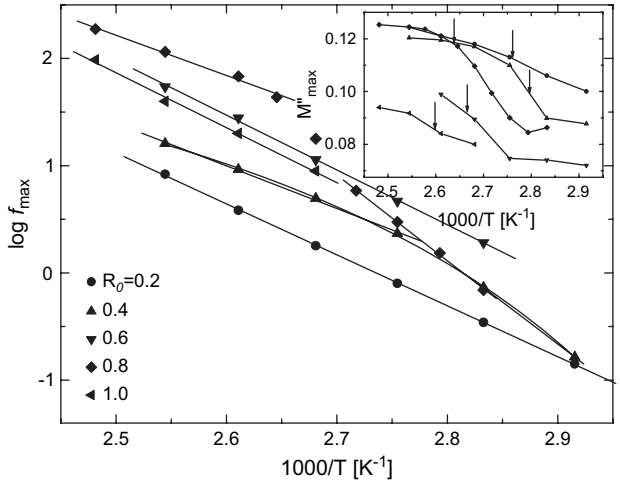

Fig. 13. Logarithm of the M'' peak frequency f_{max}, related to the conductivity, vs. inverse temperature (Arrhenius diagram). Inset shows the dependence of the magnitude of the maximum of electric modulus, M''_{max}, on the inverse temperature (arrows indicate the clearing temperatures found by DSC measurements).

Arrhenius equation with $E_a = 1.55$ and 0.79 eV and $f_\infty = 10^{22}$ and 10^{11} Hz fitted well to the data in the smectic and the isotropic phase, respectively. The corresponding values for the material with R_0 equal to 0.8 were found equal to 1.58 and 0.75 eV, and 3×10^{22} and 10^{12} Hz, respectively. The higher activation energies calculated for the smectic phase reflect the difficulty of the charge carriers to move within this phase. For the materials with $R_0 = 0.2$, 0.6 and 1.0, the Arrhenius equation was fitted in the whole temperature range with parameters 0.94, 1.0 and 1.0 eV, and 10^{13}, 10^{15} and 10^{15} Hz, respectively.

A significant change of the magnitude of the M'' maximum was observed at the clearing temperature for all the materials as can be followed in the inset of Fig. 13, where the clearing temperatures (DSC measurements) are indicated by arrows. M''_{max} increases significantly with temperature increasing to the clearing temperature and becomes almost constant in the isotropic phase. This behavior can be understood in terms of an increase in the charge carrier concentration, which contributes to conductivity, due to the increase in molecular mobility passing from the smectic to the isotropic state.

Finally we should mention that LCPBD with $R_0 = 0.4$ was used also for optical investigations at room temperature [18]. It was found that: (1) photochemically induced *trans–cis–trans* isomerization of azobenzene groupings results in their local reorientation upon irradiation with linearly polarized UV light; (2) resulting dichroism and birefringence are stable and can be erased by subsequent irradiation with non-polarized light. Further irradiation with polarized light induces anisotropy again. Points (1) and (2) suggests that LCPBDs and also linear and crosslinked materials based on these LCPBDs can be used for reversible optical data storage in photonics.

4. Conclusions

As follows from sulfur elemental analysis, ^{1}H NMR spectroscopy and GPC, comb-like LCPBDs can be prepared by addition of thiols on double bonds of PBD. It was found that ca. ~70% modification of PBD can be achieved. NMR spectroscopy has proved that the OH functionality of LCPBDs does not change in the modification. From the DSC and WAXS experiments it could be concluded that on cooling a smectic structure in the polymers is formed at 95 °C with the periodicity ~3.39 and 1.7 nm (the former value agrees well with the length of the thiol molecule). At 85 °C the crystallization starts and at 77 °C lamellar periodicities of 4.72, 2.45 and 1.7 nm, reflecting mutual ordering of grafted side chains, are formed. The amount of ordered phase in the polymers increases with increasing modification. A simple dielectric behavior with segmental α-relaxation and secondary β-relaxation was found for unmodified PBD. Two secondary β- and γ-relaxations were observed for LCPBDs and assigned to the local motion of the octyloxy end groups of the side chains, and to the motion of the azobenzene moiety of the side chain around its long molecular axis. At higher temperatures, α-relaxation was observed only for the composition with the lowest R_0 (=0.2), shifted to higher temperatures/lower frequencies with respect to unmodified PBD. We assume that α- relaxation is suppressed in the LCPBDs with higher R_0 due to a higher order of the smectic phase, formed within them. The δ-relaxation, assigned to liberation fluctuations of mesogen around the short molecular axis, was observed at temperatures higher than those of the α-relaxation in the LCPBDs with $R_0 = 0.4$, 0.6 and 0.8. Conductivity and interfacial Maxwell–Wagner–Sillars relaxation, indicating electrically heterogeneous materials due to the formation of the ordered smectic phase, were investigated by analyzing the data within the conductivity and the electric modulus formalisms. Dielectric behavior (in particular $\varepsilon'(T)$ at constant frequency), individual relaxations (α and δ) and conductivity exhibit distinct changes at the phase transition temperatures determined by DSC.

Acknowledgements

Financial support of the Grant Agency the Academy of Sciences of the Czech Republic (Grant No. IAA4112401) and of the Ministry of Education, Youth and Sports of the Czech Republic (Grant MSM 0021620835) is gratefully acknowledged.

References

[1] Gordon M, Platé NA, editors. Liquid crystal polymers II/III. Berlin: Springer-Verlag; 1984 (Adv Polym Sci 1984; 60/61).
[2] Shibaev VP, Lam L, editors. Liquid crystalline and mesomorphic polymers. Berlin: Springer-Verlag; 1994.
[3] Meier W, Finkelmann H. Makromol Chem Rapid Commun 1990;11:1253.
[4] Bladon P, Warner M. Macromolecules 1993;26:1078.
[5] Bobrovsky A, Boiko N, Shibayev V, Stumpe J. Photochem Photobiol A 2004;163:347.
[6] Schab-Balcerak E, Sapich B, Stumpe J. Polymer 2005;46:49.
[7] Tang T, Zeng F, Wu S, Tong Z, Luo D, She W. Opt Mater 2004;27:585.
[8] Han YK, Ko BS. Opt Mater 2002;21:621.
[9] Dumont M, Osman E. Chem Phys 1999;245:437.
[10] Jin S, Wübbenhorst M, van Turnhout J, Mijs W. Macromol Chem Phys 1996;197:4135.
[11] Wübbenhorst M, van Koten E, Jansen J, Mijs W, van Turnhout J. Macromol Rapid Commun 1997;18:139.
[12] Mysliwiec J, Miniewicz A, Nešpůrek S, Studenovský M, Sedláková Z. Opt Mater 2007;29:1756.
[13] Demchenko YA, Studenovský M, Sedláková Z, Šloufová I, Baldrian J, Ilavský M. Eur Polym J 2003;39:437.
[14] Jigounov A, Sedláková Z, Spěváček J, Ilavský M. Eur Polym J 2006;42:2450.
[15] McCrum NG, Read BE, Williams G, editors. Anelastic and dielectric effects in polymeric solids. Berlin: Springer-Verlag; 1991.
[16] Zentel R, Strobl G, Ringsdorf H. Macromolecules 1985;18:960.
[17] Kremer F, Schoenhals A, editors. Broadband dielectric spectroscopy. Berlin: Springer-Verlag; 2003.
[18] Rais D, Zakrevskyy Y, Stumpe J, Nešpurek S, Sedláková Z. Opt Mater, in press.
[19] Toman L, Vlček P, Sufčák M, Pleska A, Spěváček J, Holler P. Collect Czech Chem Commun 2000;65:352.
[20] Podešva J, Spěváček J, Dybal J. J Appl Polym Sci 1999;74:3214.
[21] Havriliak S, Negami S. Polymer 1967;8:161.
[22] Marquardt DW. J Soc Ind Appl Math 1963;11:431.
[23] Roper TM, Guymon CA, Jönsson ES, Hoyle CE. J Polym Sci Part A Polym Chem 2004;42:6283.

[24] Demus D, Goodby JW, Gray GW, Spies HW, Vill V, editors. Handbook of liquid crystals. Weinheim: Wiley-VCH; 1998.
[25] Govind AS, Madhusudana NV. Eur Phys J 2002;E9:107.
[26] Ferry JD. Viscoelastic properties of polymers. 3rd ed. New York: Wiley; 1980.
[27] Hofmann A, Alegria A, Colmenero J. Macromolecules 1996;29:129.
[28] Zorn R, Mopsik FI, McKenna GB, Willner L, Richter D. J Chem Phys 1997;107:3645.
[29] Schoenhals A, Carius HE. Int J Polym Mater 2000;45:239.
[30] Mano JF. J Macromol Sci Part B 2003;42:1169.
[31] Mierzwa M, Floudas G, Wewerka A. Phys Rev E 2001;64:031703.